Fabrication of fluidic devices with 30 nm nanochannels by direct imprinting

Irene Fernandez-Cuesta[a)]
DTU Nanotech, Technical University of Denmark, Building 345 East, 2800 Kgs Lyngby, Denmark and The Molecular Foundry, Lawrence Berkeley National Laboratory, 1 Cyclotron Road, Berkeley, California 94720

Anna Laura Palmarelli
Politecnico di Torino, Corso Duca degli Abruzzi, 24, 10129 Torino, Italy and The Molecular Foundry, Lawrence Berkeley National Laboratory, 1 Cyclotron Road, Berkeley, California 94720

Xiaogan Liang, Jingyu Zhang, Scott Dhuey, Deirdre Olynick, and Stefano Cabrini
The Molecular Foundry, Lawrence Berkeley National Laboratory, 1 Cyclotron Road, Berkeley, California 94720

(Received 30 June 2011; accepted 30 October 2011; published 23 November 2011)

In this work, we propose an innovative approach to the fabrication of a complete micro/nano fluidic system, based on direct nanoimprint lithography. The fabricated device consists of nanochannels connected to U-shaped microchannels by triangular tapered inlets, and has four large reservoirs for liquid input. A master silicon stamp with the multilevel structures is fabricated first, and then a negative replica is made, to be used as a stamp for ultraviolet nanoimprint lithography (UV-NIL). Afterwards, just one single UV-NIL step is necessary for patterning all the the micro and nanostructures. Furthermore, the devices are made of all-transparent materials, and the method allows flexibility for the type of substrates used. The active material (an inorganic-organic hybrid polymer) used for the fabrication of the device has been carefully chosen, so it has adequate surface properties (inert and hydrophilic) for its direct use for biological applications. Devices having 30 nm wide, 30 nm deep nanochannels have been fabricated, and the successful performance of the fluidic system and the continuity of the nanochannels have been proven by flow tests. © *2011 American Vacuum Society*. [DOI: 10.1116/1.3662886]

I. INTRODUCTION

In the last 20 years, the combination of different functionalities within the same chip has lead to development of the total analysis systems at the microscale (μTAS), or Lab-on-a-Chip.[1] The range of applications of such integrated devices is broad,[2] and, among others, life sciences have benefited the most.[3] For example, in medicine, the use of a small volume of liquid is highly desirable, because it minimizes the amount of sample necessary, and also allows for early stage detection of diseases. These platforms are portable, inexpensive, have a fast response time and a high sensitivity, need very little amount of liquid and could be used by nonexperts at the point-of-care.[4]

The key technology that enables the miniaturization of such systems is microfluidics. The fabrication of microchannels is already wide spread and a very well established technology,[5] but shrinking the dimensions of the structures down to the nanometer scale is a challenging new topic. A variety of work can be found in the literature proposing approaches to the fabrication of nanochannels.[6–8]

Here, we propose a method for the fabrication of complete micro/nanofluidic devices based on a single imprinting step. This method is not only fast and simple, but also cost effective. It presents many advantages compared to previous work: since it is based on nanoimprint lithography, multiple devices can be patterned simultaneously; no postprocessing is required, which leads to very reproducible structures; a polymer is used as active material, which is convenient to reduce fabrication costs; and it is very versatile regarding the used substrates, which can be chosen according to the specific application.

[a)]Author to whom correspondence should be addressed; electronic mail: ifernandez-cuesta@lbl.gov

II. FABRICATION

The complete approach for the fabrication of the micro/nanofluidic device is illustrated in Fig. 2, and is based on a double UV-NIL replication, as detailed next.

This fabrication method can be extended to integrate metallic sensing components, such as plasmonic antenna[9,10] or electrical contacts[11] [see corresponding schemes in Figs. 1(b) and 1(c)], as will be reported in another work.

A. Device design

The layout of the device can be seen in Fig. 1(a). It consists of two U-shaped microchannels, having two reservoirs each at the ends. Several nanochannels bridge both of them. To overcome the size difference between micro and nano channels, tapered inlets have been included in the design. These structures facilitate the use of such devices for biosensing (e.g., for DNA stretching in nanochannels[12]).

The process is done at a wafer scale level, and each silicon stamp contains up to 16 devices (1.5 cm × 1.5 cm). Multiple device geometries and configurations can be included in the same stamp. The number of nanochannels per device (from 1 up to 12), their width (from 12 nm up to 50 nm) as well as the microchannel geometry are varied from one device to another.

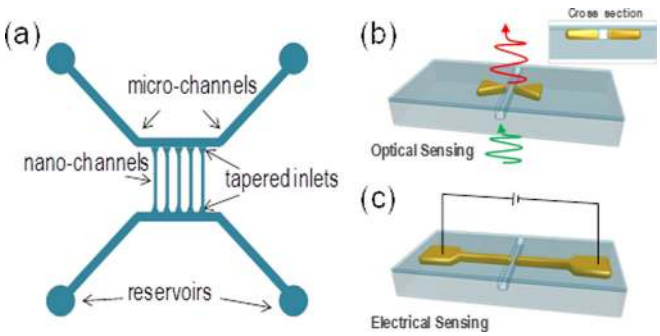

FIG. 1. (Color online) Scheme of the device geometry and performance. Panel (a) shows a scheme of the elements in the device: it is composed by two micro channels, that each have two reservoirs at the ends, and that are connected trough nanochannels. The nanochannels have triangular graded profile structures, to facilitate liquid flow. Panels (b) and (c) show two different possibilities of sensing elements—plasmonic antenna and electric contacts—made of metal, that can be integrated with the nanochannels in the device, to perform *in situ* detection (optical and electrical, respectively).

B. Silicon stamp

The fabrication of the silicon stamp is illustrated in Figs. 2(a)–(c). A (100) 4 in. silicon wafer is used as a substrate for the stamp fabrication. The nanochannels are first defined by electron beam lithography (EBL) (Vistec VB 300, 100 kV, 2000 μC/cm^2) on a 45 nm thick 950 k poly(methyl methacrylate) (PMMA) layer, and developed in an ultrasonic bath of 7:3 IPA:water solution at −5°C for 100 s. The nanochannels are etched down into the silicon with a 6 s inductive coupled plasma (ICP) reactive ion etching (RIE) (25 sccm of SF_6 and 43 sccm of C_4F_8, 30 W RF, at 20 C). The remaining PMMA is stripped in acetone [see Fig. 2(a)].

The microchannels are then patterned by photolithography: a 15 μm thick layer of a positive tone photoresist is spin-coated on the sample, the mask is properly aligned to the nanochannels and exposed for 3 s with a 17 mW/cm^2 365 nm UV-lamp. The exposed areas are developed in an alkaline aqueous solution (MAD331) for 45 s. Then, the microstructures are etched with a 2 min RIE [Fig. 2(b)], what gives a channel depth of 4 μm.

Triangular tapered inlets are milled by focused ion beam (FIB), at 30 kV, using a beam current of 200 pA [Fig. 2(c)]. To get the graded profile, a 10 μm wide, 20 μm long triangle is first milled during 120 s. Then, a trapezoid having the same base as the previous triangle, but being 1.5 μm shorter is milled for another 120 s. This process is repeated several times for shorter and shorter trapezoids, until completion of the 20 μm long structure. The short side of the trapezoid is also shortened in each step, so the graded profile is achieved not only in the direction along the nanochannel, but also in the perpendicular one.

Finally, the silicon stamp is coated with a monolayer of fluorinated silanes ((1H, 1H, 2H, 2H) tetrahydrooctyl trichlorosilane) in gas phase,[13] during 20 min in a vacuum oven at 80 °C.

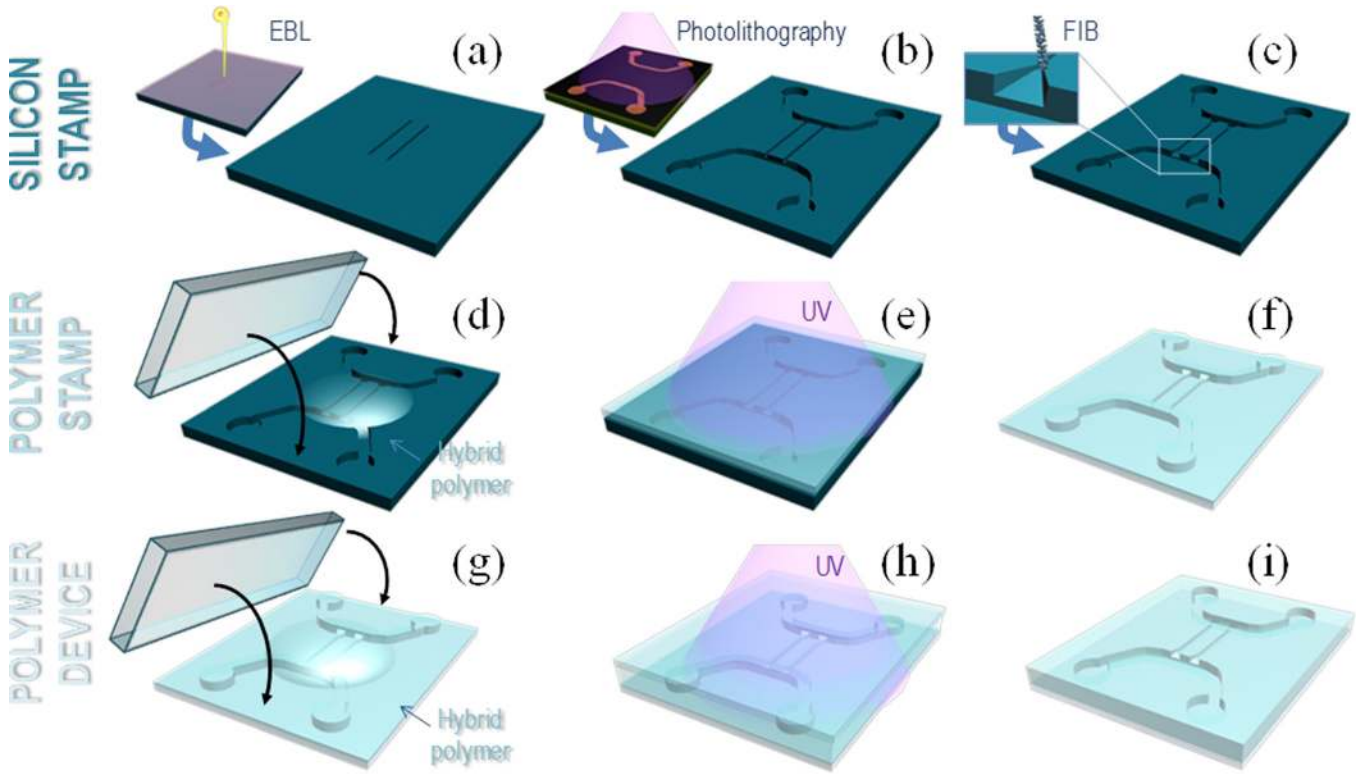

FIG. 2. (Color online) Scheme of the fabrication process. A master stamp is first fabricated in a silicon wafer. The nanochannels are defined by EBL and ICP RIE (a), the microchannels by photolithography and RIE (b) and tapered inlets are milled by FIB (c). A drop of a UV-curable inorganic-organic polymer (Ormostamp) is cast on the silicon stamp (d), pressed with a transparent substrate and cured with UV light (e), so a negative replica in transparent materials is fabricated (f). Finally, we repeat the same UV-NIL process (g), (h) to get the final structures made of polymer on a transparent substrate (i).

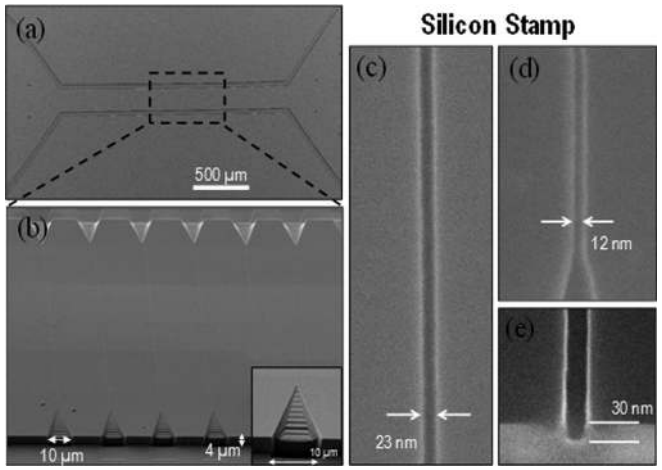

FIG. 3. Silicon stamp images. A general overview of a device and the microchannels can be seen in panel (a). The nanochannels connected to the microchannels via triangular tapered inlets are shown in panel (b), and a detail of one of the three-dimensional structures is shown in the inset. Detailed images of two nanochannels, 23 nm and 12 nm wide can be seen in panels (c) and (d), respectively. A cross section of a 30 nm deep nanochannels is shown in panel (e).

Figure 3 shows images of the silicon stamp. A general overview of one of the devices is shown in Fig. 3(a), where the microchannel distribution can be seen. Figure 3(b) shows a closer view of the area where the nanochannels lie. The nanochannels are 150 μm long, and are perpendicular to the microchannels. The tapered inlets (see the inset of the figure) can also be seen. Figures 3(c) and 3(d) show details of two nanochannels, that are 23 nm and 12 nm wide respectively. In Fig. 3(e), a cross section of a nanochannel can be seen, where a depth of 30 nm has been measured.

The stamp fabrication is complex, and requires several steps, some of them being challenging (e.g., the nanochannels patterning, due to the small feature size), and others being time consuming (e.g., the fabrication of each tapered inlet requires 35 min of milling time, besides the necessary alignment). In addition, these devices are aimed at biological applications, where optical performance is necessary, so samples made of all-transparent materials are highly desirable. For all these reasons, a parallel high throughput replication method, such as nanoimprint lithography (NIL),[14–16] and more specifically UV-NIL[17] is very convenient, since it allows to replicate this three-dimensional multilevel multisize stamp easily in one single step on a transparent substrate. The same silicon stamp can be used to fabricate multiple copies and a larger number of devices.

C. Double replication process

A negative replica of the silicon master needs to be fabricated first, to be used as a stamp for a second imprinting step.

The fabrication of the negative replica is schematized in Figs. 2(d)–(f). A fused silica substrate is dehydrated at 180 °C for 30 min, spin coated with an adhesion promoter (*Ormoprime*, from *micro resist technology, GmbH*) at 3000 rpm and baked at 150 °C for 5 min. A 150 nm thin layer is obtained. Then, a drop of *Ormostamp* (an inorganic-organic tailored flexible hybrid polymer, also from *micro resist technology, GmbH*)[18–20] is cast on the fused silica substrate. A volume of ~2 μL of Ormostamp per fabricated device is used. The substrate is then brought into contact with the silicon stamp [Fig. 2(d)]. No external pressure is applied. The stamp-polymer-substrate sandwich is heated on a hot plate at 100 °C to for 2 mins, what decreases the liquid viscosity from 0.545 Pa s at room temperature, down to 0.002 Pa s at 100 °C. The viscosity at 100 °C has been obtained by extrapolation: micro resist technology measured viscosities of 545 mPa s, 400 mPa s and 150 mPa s at 21 °C, 30 °C and 50 °C, respectively. We fitted these data to a log(η) versus 1/T plot, and extrapolated the get a viscosity of 2 mPa s at 100 °C. This baking step helps the material to flow into the smallest structures, improves the adhesion to the substrate and creates a more homogeneous layer. Then, it is cured for 120 s with UV light (365 nm, 17 mW/cm^2) [Fig. 2(e)]. After a post-baking of 10 min at 180 °C, the stamp and the substrate are gently separated [Fig. 2(f)].

Figure 4 shows images of the polymeric negative replica. A general overview of the micro/nanochannels and the inlets can be seen in Fig. 4(a). A tapered inlet together with its partial profile are shown in Fig. 4(b), and an AFM image and the corresponding profile of a 30 nm wide nanochannel are shown in Figs. 4(c) and 4(d), respectively.

We have chosen *Ormostamp* as material to fabricate the negative replica for various reasons. First of all, it is transparent to the UV light even after cured, which is necessary for its use as a stamp in the second UV-NIL step. Also, because the cosslinked material contains SiO_x, it can be coated with a monolayer of fluorinated silanes to improve the releasing properties for subsequent imprinting steps. Furthermore, the cured material is hard (modulus of elasticity of 0.6 G Pa), and mechanically stable, even at high temperatures. The stability and mechanical properties of the material allows to use the Ormostamp-stamps for doing multiple imprints (> 50). More information about the chemistry, composition, and surface properties of Ormostamp can be found in the works by Klukowska *et al.*[18–21]

The final structures are patterned following the same replication process, using the negative replica as a stamp. The steps of the fabrication are summarized in Figs. 2(g)–(i). The adhesion promoter is spin coated on a glass slide, then the liquid *Ormostamp* material is cast [Fig. 2(g)] and imprinted with the negative replica [Fig. 2(h)] following the same procedure as before. After stamp release, we obtain the micro/nano fluidic system fabricated in a polymer [Fig. 2(i)] on a transparent glass slide.

Figure 5 shows images of the structures of one of the devices. A general overview of the micro and nanochannels and the tapered triangles made of polymer can be seen in Fig. 5(a). Figure 5(b) shows a detail of the inlets, and Fig. 5(c) an AFM image of a nanochannel, 30 nm wide.

We have chosen the same material (*Ormostamp*) to fabricate the final device because, compared to other materials (such as thermoplastic polymers used for thermal NIL) it is stable at high temperatures (up to 270 °C), so temperature is

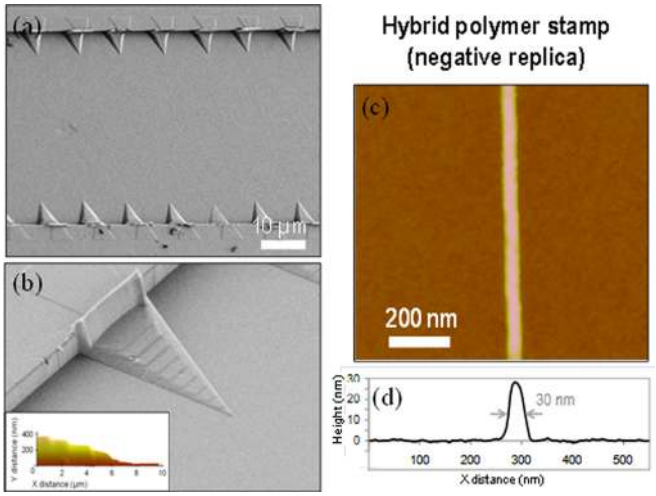

FIG. 4. (Color online) Images of the polymer replica. (a) shows several tapered inlets and part of the microchannels. A detail of one of the three-dimensional structures can be seen in panel (b), with a partial profile (8 μm long) of the structure in the figure inset. An AFM image of a nanochannels, 30 nm wide, with its corresponding profile are shown in panels (c) and (d), respectively.

not a restriction for further performance or additional post processing of the samples. Also, it is more hydrophilic than other UV-curable materials. It has a contact angle of 60° after curing, and of 15° after a 1 min UV-Ozone treatment for surface activation. Furthermore, it has an inert surface (no functional groups),[21] which makes it suitable to use the device for biosensing, where biological serum or living organisms would be flown.

It should be highlighted that this process is very versatile regarding the substrate used for the fabrication of the final device. The fact that the process is based on a casting-curing method, and that the negative stamp is already UV transparent allows the use of any other type of substrate (not necessarily transparent, nor flat) owing to the application requirements. In the work presented here, we have mainly used microscope slides, since they are cheap and adequate to be mounted and

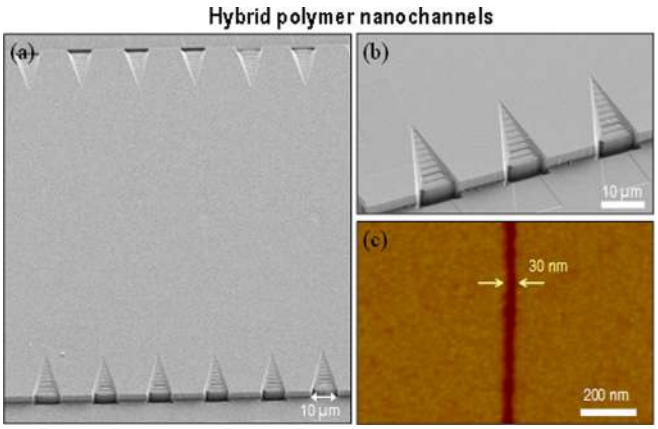

FIG. 5. (Color online) Images of the final device made by UV-NIL on a transparent inorganic-organic polymer. (a) shows a general view of a device. (b) shows details of the 3D tapered inlets, and (c) shows an AFM image of a channel, 30 nm wide.

held under a microscope for future applications where this is needed.

The main advantage of this method is its simplicity: once the stamp is fabricated, just one single UV-NIL step is required to pattern all the micro/nano structures. In addition, since there is no post processing, the dimensions of the nanochannels are very reproducible, and the presence of defects is negligible (given that they are not present in the stamp). This is an advantage compared to other works, where, even if NIL-based, the imprinted structures are used as a mask for pattern transfer into the substrate, so the final results may not be so reproducible, especially regarding the smallest structures.

1. Critical dimensions conservation during the process

One of the major issues of the process is the conservation of the lateral dimensions of the nanochannels. Thus, the width of the channels has been evaluated after every step. We have observed that the most problematic one is the anti sticking coating of the negative replica: silane molecules tend to create aggregates in the corners of the structures, increasing the width of the channels (between 15 nm and up to 50 nm in the worst case) and the surface roughness. Sonicating should be avoided to prevent peeling, and just rinsing the sample with different types of solvents after the treatment does not seem to be enough to clean the residues (not covalently bonded molecules). Luckily, we found that the material is gradually removed after using the negative stamp for imprinting. We have seen that after four dummy imprints, the channels recover the width from before the treatment, and that the roughness decreases dramatically. The dimensions and topography do not change with further imprints, so we assume that all the noncovalently bonded material is fully removed at that point. Table I summarizes the values of the surface roughness (root mean square, rms) and some geometrical parameters (width and height or depth, as corresponds) for different steps of the fabrication process evaluated from AFM images obtained using super sharp tips (radii $<$10 nm).

After all the process optimization, complete devices made of polymer, containing 30 nm wide, 30 nm deep nanochannels can be fabricated in a routine way, starting with 23 nm nanochannels on the stamp [see the results shown in Fig. 5(c)].

D. Final device

Before the structures can be used for fluidic applications, reservoirs for liquid input need to be fabricated, and finally bonded to a coverslip, to seal the channels.

For the fabrication of the four reservoirs, the sample is covered with a protective layer (15 μm of MAD1215 photoresist) on the structures side. Large holes ($\sim$1 mm diameter) are drilled all the way through the substrate by sandblasting from the other side.

Before the bonding step, the glass coverslip and the sample are cleaned with acetone and rinsed with isopropanol and methanol, to remove the photoresist and any possible contamination or residues. Then, they are treated in a UV-Ozone

TABLE I. Values of the surface roughness (RMS) and geometrical parameters (height or depth, and width) of various nanochannels in the different fabrication steps.

	RMS (nm)	Height or Depth (nm)	Width (nm)[a]	Width (nm)[b]
Silicon stamp	0.471	30	37	23
Polymer stamp	0.205	30	40	26
Polymer stamp (after antisticking coating)	1.09	33	60	40
Imprinted nanochannels (imprint n° 1)	1.19	30	55	38
Imprinted nanochannels (imprint n° 4)	0.459	29	39	30

[a]Width of a nanochannel that was initially 37 nm wide in the stamp.
[b]Width of a nanochannel that was initially 23 nm wide in the stamp.

chamber for 2 mins, for surface activation. The UV-Ozone activates the Ormostamp surface by creating a large number of –OH groups.[21] This not only improves the hydrophilicity of the surface, but also improves the bonding process. Finally, they are brought into contact and pressed together. We believe that the bonding mechanism involves the formation of strong intermolecular bonds from the hydroxyl groups of the glass coverslip and the samples' treated surface. This mechanism is well-known in PDMS-to-glass or PDMS-to-PDMS bonding, where the same processes occur.[22]

III. FLOW TEST

To evaluate the continuity of the 30 nm wide, 30 nm deep, 150 μm long nanochannels, flow tests have been performed. An inverted microscope (Olympus IX-81) has been used. The *bright field* and/or *fluorescence* images are studied using an Andor MMCCD camera, by illuminating with white light from above or by exciting from underneath using an adequate filter set, respectively.

The flow has been studied using different types of liquids such as DI water, saline aqueous solutions $0.5 \times$ TBE (0.045 M tris-base, 1 mM EDTA, 0.045 M boric acid) and ethanol. These were stained with Alexa Fluor 647 ($\lambda_{ex} = 650$ nm; $\lambda_{em} = 668$ nm) for fluorescent characterization.

It is very challenging to observe the nanochannels directly due to their very small dimensions. Instead, the triangular tapered structures at the ends are easy to see and they get filled very quickly when there is a liquid flow along the nanostructures.

We have observed the liquid flowing by capillarity under different hydrostatic pressure conditions: one or two reservoirs, both at opposite sides of the same microchannel, have been filled with liquid. We have seen that when 5 μL of

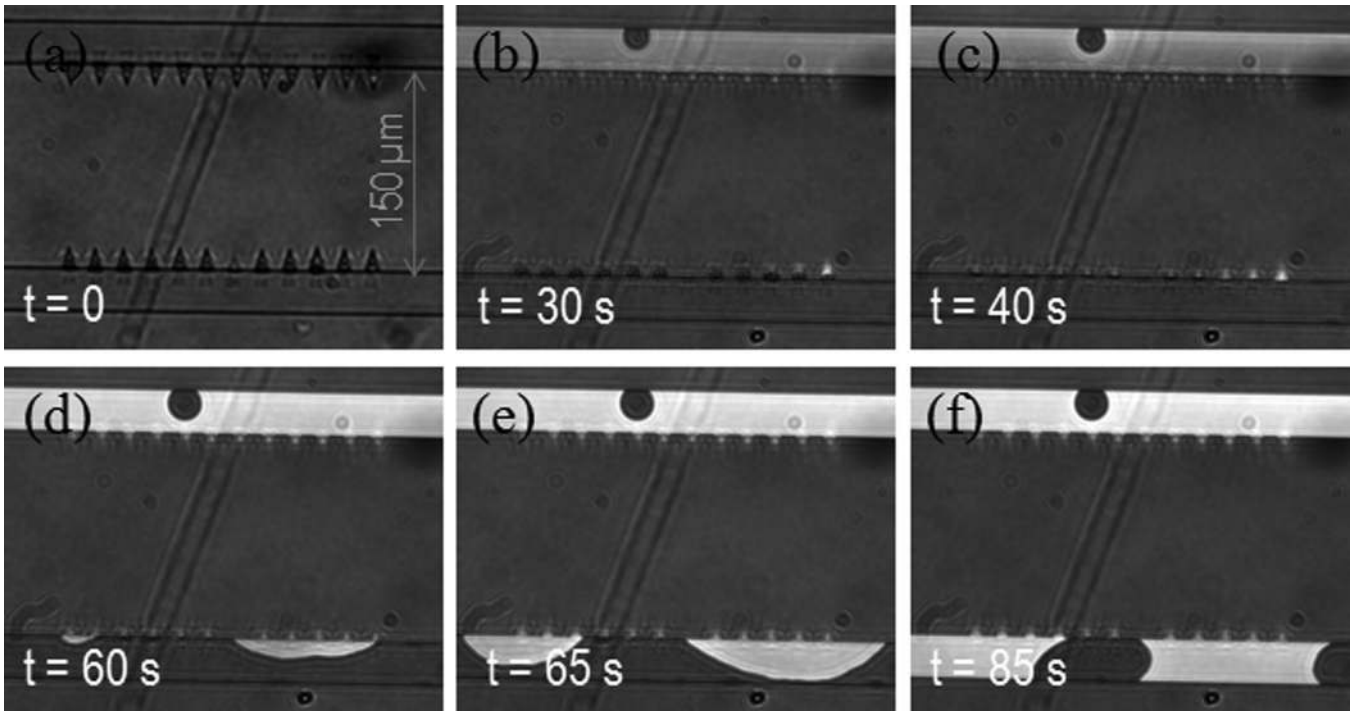

FIG. 6. Bright field images of a flow test. (a) shows the sample's topography: two horizontal microchannels are connected by 12 perpendicular nanochannels. The triangular tapered inlets can be clearly seen. (b) 5 μL of Alexa Fluor stained ethanol are inserted in the top right reservoir. The liquid flows along the microchannel, and some liquid accumulation can be seen in the triangular structures at the other side of the nanochannels, as an indication of the existence of flow. The triangular structures are gradually filled from right to left (c). (d) another 5 μL of stained (higher concentration than before) liquid are inserted in the opposite reservoir (upper left one). After few seconds, the liquid starts to fill the microchannel (d), (e), as a consequence of the hydrostatic pressure exerted by the liquid drops on the reservoirs. In less than 1 min, the microchannel is filled with the liquid that has flown across the nanostructures (f).

liquid are pippeted in only one of the reservoirs, the microchannel is filled, and a small accumulation of liquid is observed at the other end of the nanochannels: small liquid bubbles appear in the triangular inlets. However, the hydrostatic pressure is not enough to push the liquid to fill the other microchannel, not even for the lowest surface tension liquid used (ethanol). When both reservoirs at the ends of the same microchannel are filled with liquid (5 μL in each), the hydrostatic pressure is enough to push the liquid along the nanochannels, and to fill the other microchannel, as can be seen in the stack of bright field images in Fig. 6. Here, 5 μL of liquid (5 mg/mL solution of Alexa Fluor 647 in ethanol) were inserted in the reservoir connected to the microchannel in the upper-right part of the image. After a few seconds (enough to fill the microchannel completely), another 5 μL of more concentrated solution (10 mg/mL) was put in the opposite reservoir connected to the same microchannel, in the upper left part of the image. It can be seen how the liquid flows along the nanochannels, as the tapered structures at the opposite side become bright. After tens of seconds, the liquid accumulates, and finally fills the microchannel.

Figure 7 shows fluorescent images. Figure 7(a) corresponds to a similar sample and under similar conditions to those previously shown in Fig. 6. Here, owing to the high contrast observed, we assume that there is no leaking, and that the liquid flows just through the nanochannels. Figure 7(b) shows a triangular inlet and a 30 nm nanochannel. Figure 7(c) shows a detail of three nanochannels of different widths: 35 nm, 30 nm and 27 nm from left to right. A fluorescence intensity profile is shown in Fig. 7(d), obtained after integration along the nanochannels axes from Fig. 7(c).

These results show the successful performance of the imprinted fluidic system and prove the continuity of the nanochannels. Future works may range from biological applications, DNA stretching in such small structures or to the integration of different sensing or actuating elements within the same device.

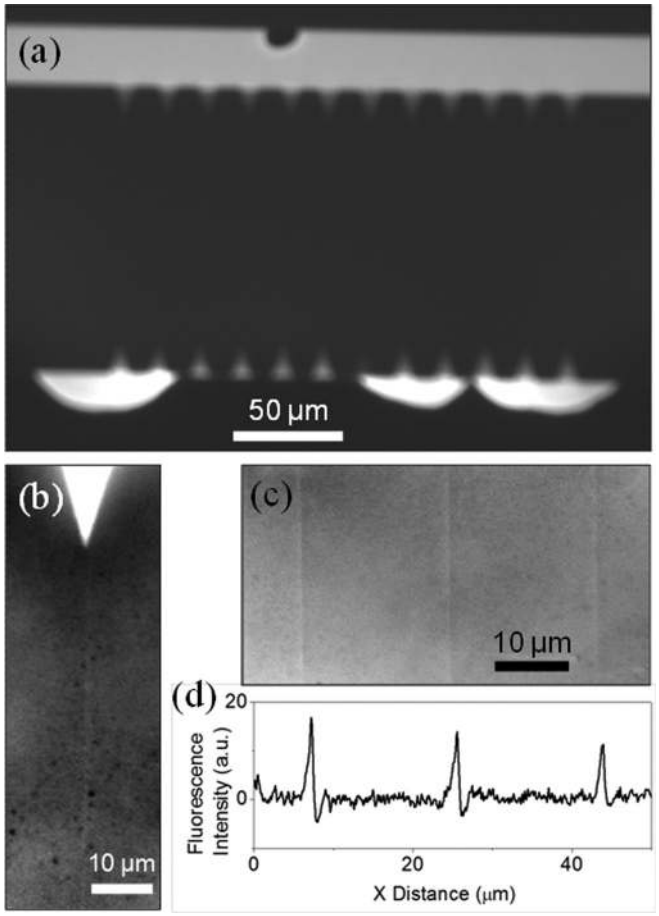

FIG 7. Filtered fluorescence images of a flow test, obtained by filling the two upper reservoirs with 5 μL of Alexa Fluor stained ethanol. (a), general overview of the microchannels, tapered inlets and nanochannels (that run in vertical direction, but due to contrast issues are not visible). No liquid leaking is observed outside the micro or the nanochannels. (b) shows a detail of a tapered triangle and a nanochannel. (c) shows nanochannels with three different lateral dimensions (35 nm, 30 nm and 27 nm, from left to right). A fluorescence intensity profile of (c) is shown in panel (d), obtained after integrating the signal along the nanochannels axis.

IV. SUMMARY AND CONCLUSIONS

We have presented a complete approach for the fabrication of functional devices with micro and nanochannels, connected by three-dimensional tapered inlets, and macro reservoirs, made of transparent materials.

We have shown the different steps for the fabrication of the master silicon stamp, including patterning of sub-20 nm nanochannels, U-shaped microchannels and tapered triangular structures. We have also shown the fabrication by UV-NIL of a transparent negative replica, and the results of the final device, made by one single UV-NIL step in a transparent inorganic-organic co-polymer, with very convenient surface properties. The challenges of the replication process have been discussed, and, after optimization, we have shown that we can fabricate 30 nm wide nanochannels in a routinely way.

Finally, the good performance of the fluidic structures and the continuity of the nanochannels have been proven by flow tests using different stained liquids by fluorescence microscopy.

ACKNOWLEDGMENTS

I.F. wants to acknowledge the EC Marie Curie Research Training Fellowship (Grant No. PIOF-GA-2009-254498) for financial support. The authors also want to acknowledge Gabi Gruetzner for fruitful discussions and useful feedback about the materials properties. This work was performed at the Molecular Foundry, Lawrence Berkeley National Laboratory, and was supported by the Office of Science, Office of Basic Energy Sciences, Scientific User Facilities Division, of the U.S. Department of Energy under Grant No. DE-AC02—05CH11231.

[1]A. Manz, N. Graber and H. M. Widmer, Sens. Actuators B **1**, 244 (1990).
[2]P. Abgrall and N. T. Nguyen, Anal. Chem. **80**, 2326 (2008).
[3]P. Yager, T. Edwards, E. Fu, K. Helton, K. Nelson, M. R. Tam, and B. H. Weigl, Nature **442**, 412 (2006).
[4]L. Gervais and E. Delamarche, Lab. Chip. **9**, 3330 (2009).
[5]G. M. Whitesides, Nature **442**, 368 (2006).

[6]X. Liang, K. J. Morton, R. H. Austin, and S. Y. Chou, Nano Lett. **7**, 3774 (2007).
[7]S.-m. Park, Y. S. Huh, K. Szeto, D. J. Joe, J. Kameoka, G. W. Coates, J. B. Edel, D. Erickson, and H. G. Craighead, Small **6**, 2420 (2010).
[8]D. Mijatovic, J. C. T. Eijkel, and A. van den Berg, Lab. Chip. **5**, 492 (2005).
[9]J. N. Anker, W. P. Hall, O. Lyandres, N. C. Shah, J. Zhao, and R. P. Van Duyne, Nature Mater. **7**, 442 (2008).
[10]N. Liu, M. L. Tang, M. Hentschel, H. Giessen, and A. P. Alivisatos, Nature Mater. **10**, 631 (2011).
[11]X. Liang and S. Y. Chou, Nano Lett. **8**, 1472 (2008).
[12]H. Cao, J. Tegenfeldt, R. Austin, and S. Chou, Appl. Phys. Lett. **81**, 3058 (2002).
[13]M. Beck, M. Graczyk, I. Maximov, E. L. Sarwe, T. G. I. Ling, M. Keil, and L. Montelius, Microelectron. Eng. **61-62**, 441 (2002).
[14]S. Y. Chou, P. R. Krauss, and P. J. Renstrom, J. Vac. Sci. Technol. B **14**, 4129 (1996).
[15]S. Y. Chou, P. R. Krauss, and P. J. Renstrom, Science **272**, 85 (1996).
[16]H. Schift, J. Vac. Sci. Technol. B **26**, 458 (2008).
[17]J. Haisma, M. Verheijen, K. van den Heuvel, and J. van den Berg, J. Vac. Sci. Technol. B **14**, 4124 (1996).
[18]A. Klukowska, A. Kolander, I. Bergmair, M. Mühlberger, H. Leichtfried, F. Reuther, G. Grützner, and R. Schöftner, Microelectron. Eng. **86**, 697 (2009).
[19]M. Mühlberger, I. Bergmair, A. Klukowska, A. Kolander, H. Leichtfried, E. Platzgummer, H. Loeschner, C. Ebm, G. Grützner, and R. Schöftner, Microelectron. Eng. **86**, 691 (2009).
[20]H. Schift, C. Spreu, M. Saidani, M. Bednarzik, J. Gobrecht, A. Klukowska, F. Reuther, G. Gruetzner, and H. H. Solak, J. Vac. Sci. Technol. B **27**, 2846 (2009).
[21]A. Klukowska, M. Vogler, A. Kolander, F. Reuther, G. Gruetzner, M. Muehlberger, I. Bergmair, and R. Schoeftner, Proc. SPIE **6792**, 67920J (2008).
[22]S. Bhattacharya, A. Datta, J. M. Berg, and S. Gangopadhyay, J. Microelectromech. S. **14**, 590 (2005).